Monte Carlo simulation of the electronic portal imaging device using GATE

Yong Hyun Chung, Cheol-Ha Baek, Seung-Jae Lee

Dept. of Radiological Science, Yonsei University College of Health Science

정용현, 백철하, 이승재

연세대학교 보건과학대학 방사선학과

Abstract

In this study, the potential of a newly developed simulation toolkit, GATE for the simulation of electronic portal imaging devices (EPID) in radiation therapy was evaluated by characterizing the performance of the metal plate/phosphor screen detector for EPID. We compared the performances of the GATE simulator against MCNP4B code and experimental data obtained with the EPID system in order to validate its use for radiation therapy.

<요 약>

새로 개발된 몬테칼로 모사코드인 GATE의 방사선치료 분야에의 적용성 검토를 위하여 방사선치료 오차확인용 전자포탈영상장치에 사용되는 금속판/형광스크린 계측기의 특성을 예측 및 분석하였다. GATE를 이용하여 계산한 6 MV 선형가속기에서 발생되는 엑스선의 에너지 스펙트럼을 바탕으로, 여러 가지 두께의 금속판/형광스크린에 대하여 계측효율과 공간분해능을 계산하였고, 이를 범용으로 사용되는 MCNP4B 모사 결과 및 실험 결과와 비교하여, 방사선치료 분야에 응용 가능성을 검증하였다.

Key word Monte Carlo simulation, GATE, EPID, LINAC

Ⅰ. Introduction

Radiation therapy is the most common method of treating cancer among the several treatment options for cancer. The goal of radiation therapy is to deliver a prescribed dose as accurately as possible to a tumor region while minimizing the dose distribution to the neighboring normal tissues [1]. The standard course of treatment is divided into daily fraction of about 2 Gy dose, delivered over a period of 5~7 weeks for a total of 50 to 70Gy cumulative dose [2]. Because of daily treatment, discrepancies in field placement occur frequently by patient movement, improper placement of shielding blocks, shifting of skin marks relative to internal anatomy and incorrect beam alignment [3].

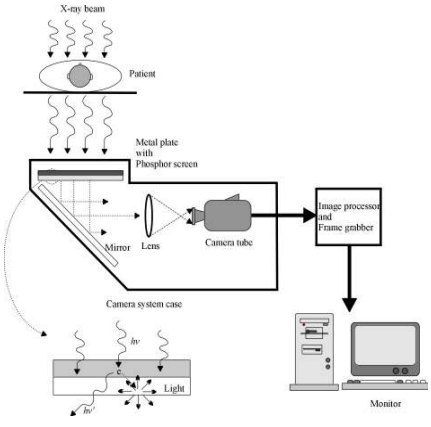

Fig. 1. Schematic diagram of video camera based EPID

Therefore, the frequent monitoring methods of patient positioning are needed to reduce the frequency of these discrepancies. Portal imaging is a process to form an image of the patient during radiation treatment for ensuring that the correct region of the patient receives the radiation therapy and that the surrounding tissues are spared. The video camera or CCD-based electronic portal imaging device (EPID) is still the most popular detector system among various EPIDs [4-7]. (Fig. 1) The x-ray detector consists of a metal plate and a phosphor screen. The metal plate generates high energy electrons when irradiated by therapeutic x-ray with energy in order of 4 ~ 25 MV, the phosphor screen converts electrons into visible light, and the light diffuses through the screen and exits the rear surface of the x-ray detector which is viewed by video camera via a 45mirror. The video signal is digitized and the digitized image can be viewed on a monitor. Metal plate/phosphor screen is largely responsible for the total performance of the EPID because it is the first stage of transferring an anatomical information in the image chains of system. Therefore the optimal design of the metal plate/phosphor screen as an x-ray detector for EPID is needed. Monte Carlo simulations are essential tools to assist in designing new medical imaging devices and optimizing data acquisition protocols. In this work, we presented the use of the GATE (Geant4 Application for Tomographic Emission) Monte Carlo platform [8-9] to perform simulations of EPID. Two quantities, such as detection efficiency and spatial resolution, were considered as a touchstone of good performance. The mega-voltage x-ray spectrum from 6 MV linear accelerator (LINAC) and the characteristics of the metal plate/ phosphor screen have been investigated. We compared the performances of the GATE simulator against Monte Carlo N-Particle, version 4B (MCNP4B) code [10] and experimental data obtained with the EPID system in order to validate its use for radiation therapy.

Ⅱ. Materials and Methods

1. X-ray Beam of Clinical LINAC

For the treatment of deep-seated tumors, mega-voltage x-rays in the range of 4 to 25 MV are used. LINAC is the most popular device for this application [11]. The energy spectrum of bremsstrahlung x-ray produced by the clinical LINAC is difficult to measure directly because detectors sensitive to photon energy cannot be used in the high photon flux produced by the accelerator. The bremsstrahlung spectrum from LINAC was obtained by using GATE code. The simulation geometry and dimensions of LINAC were designed based on the accurate geometrical data of 6 MV LINAC (Siemens, Mevatron KD) to match the actual experimental setup. This consisted of an electron beam, a shielded and water- cooled gold target, a stainless steel flattening filter and ion chambers. For the incident electron beam, a 5-deg cone-shaped with kinetic energy of 5.58 MeV, incident perpendicularly on the target was considered. The emerging photons were collected into ten energy bins, each of width 0.558 MeV, at a distance 100 cm from the target. The energy spectrum was computed by multiplying the number of photons in a given bin by the energy at the center of the bin.

To confirm the GATE simulation result, MCNP4B code was used for the same conditions and Schiff spectrum was also calculated using the following equation [12]. This is a relatively simple analytical form and has been used extensively for estimating the spectrum shape from a high energy accelerator.

$$\Gamma_{\text{Schiff}}(E_0, h\nu) = 8\left[2\left(1-\frac{h\nu}{E_0}\right)(\ln\varepsilon - 1) + \left(\frac{h\nu}{E_0}\right)^2\left(\ln\varepsilon - \frac{1}{2}\right)\right] \quad 1.1$$

$$\varepsilon = \left[\left(\frac{\mu h\nu}{2E_0E}\right)^2 + \left(\frac{Z^{\frac{1}{3}}}{C}\right)^2\right]^{-\frac{1}{2}} \quad 1.2$$

where

E_0 : total energy of incident electron [MeV]

E : scattered electron total energy [MeV]

h : bremsstrahlung photon energy [MeV]

μ : rest energy of electron [0.511 MeV]

Z : atomic number of target material

C : dimensionless constant

2. Detection Efficiency

In this study, the detection efficiency is defined as the total absorbed energy in the phosphor screen per incident x-ray. Sincethe number of optical photons generated is directly proportional to the total absorbed energy in a given phosphor screen.

In order to determine the energy absorption within the phosphor screen, GATE and MCNP4B codes were used. The x-ray detector was simply modeled, which consisted of copper plate (0~50 mm) in contact with Gd_2O_2S layer (0.3mm). Despite of complexity of phosphor screen material composition, the density of Gd_2O_2S, which is assumed to be homogeneous mono-layer, was reduced to 3.67g/㎤ accounting for polyurethane polymer-binder and small air pockets within a realistic phosphor layer [13-14]. For the incident x-ray beam, a pencil beam with bremsstrahlung spectrum as calculated in the above section, incident perpendicularly on the x-ray detector was considered. Locally distributed energy absorption was estimated in cubic cells of phosphor layer in both simulations. The total absorbed energy was computed by adding the absorbed energy in a given cell.

3. Spatial Resolution

To fully characterize the detector behavior it is necessary to have a model of optical photon transport out of the phosphor screen. The spatial resolution is defined by the full width at half maximum (FWHM) of a point spread function, which is the distribution of the optical photon-flux over the surface of the phosphor screen opposite to metal side. It is assumed that the optical photon generated in the center of a small cubic box of which total intensity is proportional to the total absorbed energy in the box and then propagates isotropically. The optical photon-flux collected over the solid angle of a rectangular pixel of size $2X \times 2Y$ can be expressed by [15-17],

$$P(z) = \int_{-Y}^{Y}\int_{-X}^{X} \frac{N_{opt}}{4\pi} \times \frac{z}{\left(x^2 + y^2 + z^2\right)^{3/2}} dx\,dy \quad 3.1$$

where x, y and z are 2-dimensional coordinates of the end-sided phosphor screen and distance to the light source, respectively. N_{opt} is the number of photons generated at which the x-ray energy is absorbed within phosphor screen and can be calculated by

$$N_{opt} = \varepsilon \times \frac{E_{abs}}{E_{opt}} \quad 3.2$$

In Eq. 3.2, is the intrinsic conversion efficiency in the range of 15~20 % [18-19], E_{opt} and E_{abs} are the optical photon energy (2.28 eV for 545 nm wavelength from Gd_2O_2S:Tb) and the locally absorbed energy within phosphor screen from the secondary fast electrons, respectively.

Locally distributed energy absorption was estimated in 100×100×100㎛³ cubic cell of phosphor layer by GATE and MCNP4B simulations as described in the previous section. Then, the center point of the cell was assumed to be the representative position as the optical photon-source point. Based on the Monte Carlo simulated spatial distribution of energy absorption, the distribution of optical photon flux collected by 10×10 ㎛² pixel area as a function of pixel position on the free surface of the phosphor screen was calculated by Eq. 3.1 and Eq. 3.2 using a hand-made C program.

To confirm the simulated spatial resolution, the experimental measurement was carried out. The line spread function is equal to the integral of the point spread function and the derivative of the edge spread function [20]. To determine the edge spread function of

metal plate/phosphor screen, a density profile of a film across an edge was measured. A lead block with dimensions of 20×10×5㎤ was placed on a film cassette and across half of the x-ray field of 6 MV LINAC (Siemens, Mevatron KD) with 167 cm SSD. The 135mg/㎠-coverage Lanex screen attached onto a 2mm-thick copper plate was placed in the film cassette with the phosphor layer of the detector in contact with the portal film (Kodak, X-Omat V film) which is commonly used for the therapy verification. The film was exposed by the x-ray intensity of 50 MU (Monitor Unit, 1MU may be calibrated to equal 1 cGy at 100 cm SSD for a 10×10㎠ field size at 5 cm-depth in water). The shape of the edge spread functions were measured with film digitizer passing through the image of the edge, perpendicular to the edge length. Thirty scans were made and these scans were averaged together to reduce uncertainty in the final estimation of the edge spread function.

Ⅲ. Results and Discussions

1. Bremsstrahlung Spectrum

Simulated bremsstrahlung intensity by GATE and MCNP4B and Schiff intensity spectrum were represented in **Fig.2**. The mean energy of the bremsstrahlung x-ray is 1.57 MeV. As shown in **Fig.2**, the GATE simulation result provides reasonable agreement with MCNP4B simulation and a theoretical model. The normalized number spectrum is, then, implemented to the source input of Monte Carlo simulation for estimating the detection efficiency of metal plate/phosphor screen detector.

2. Detection Efficiency

For the incident bremsstrahlung x-ray with the mean energy of 1.57 MeV, the detection efficiency is shown in **Fig.3** in unit of percentage for the 0.3 mm-thick phosphor screen as a function of the metal thickness. The result shows that the GATE provides reasonable agreement with MCNP4B within 5% error. The detection efficiency rapidly approaches to the maximum value at a range of 1.5 ~ 2.0 mm of metal thickness and then decreases very slowly as the metal thickness increases. This characteristic can be analyzed by the electron flux emitted from the metal plate and the electron path length in the phosphor screen [21]. The number of electrons penetrating metal plate depends upon their energies and corresponding path lengths, so that the total absorbed energy distribution in the phosphor screen as a function of metal thickness shows a maximum value.

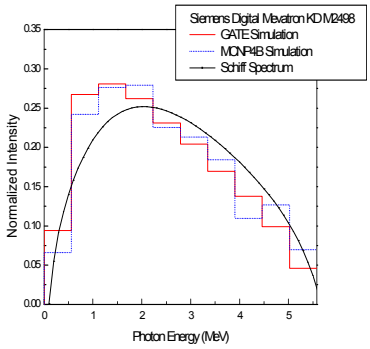

Fig. 2. Simulated bremsstrahlung intensity by GATE (line histogram) and MCNP4B (dot histogram) and Schiff intensity (line) spectrum were represented.

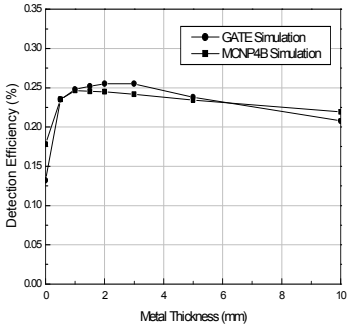

Fig.3. Detection efficiency for 0.3 mm-thick phosphor as a function of the metal thickness.

The distribution of the optical photon flux collected by 10×10㎡ pixel area on the free surface of the phosphor screen as function of the pixel position was simulated for 0.3 mm-thick phosphor layer with 2.0mm

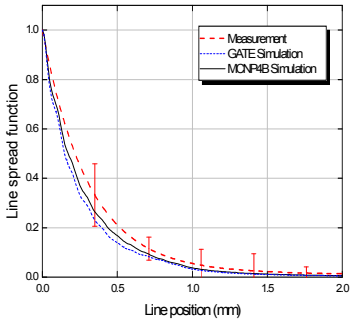

Fig. 4. Measured and simulated line spread functions of the 2 mm-thick copper plate and 0.3 mm-thick phosphor screen.

3. Spatial Resolution

thickness of the metal plate. To quantify the spatial resolution, the edge spread function was fitted with the second-order exponentially decay curve as obtained from portal film. For comparing the measured edge spread function and the calculated point spread function, these are converted into line spread functions by differentiation and integration, respectively. Three line spread functions obtained by GATE, MCNP4B and measurement are shown in **Fig.4**, and are agreed well to each other in error boundaries. The FWHMs of the line spread functions appear to be 0.34 mm and 0.43 mm, for simulation and measurement, respectively. Unlike the simulation model, the phosphor screen is supported on a plastic support [22] and is bonded to the metal plate by plastic tapes so that the phosphor is not in direct contact with the metal plate in measurement. Also the scattering effects of the incident x-ray by surrounding materials including the film cassette were not considered in simulation. Since the high energy electrons emitted from the metal plate can spread in the plastic support and tapes before entering the phosphor and the film can be exposed by the scattered radiation, so that the measured FWHM is lager than the simulation one.

VI. Conclusion

We have validated the use of GATE, a newly developed Monte Carlo code for the simulation of medical imaging systems, for radiation therapy application by demonstrating the feasibility and accuracy of performing a simulation of EPID system. The bremsstrahlung spectrum from clinical LINAC and the detection efficiency as well as the spatial resolution for various combinations of metal plate /phosphor screen as a detector of video camera-based EPID were estimated by GATE simulation and verified by MCNP4B simulation and the experimental measurements. This result can be used to determine the optimal thickness of metal plate and phosphor screen for specific application. The good agreement between GATE, MCNP4B simulated and measured results supported the potential of GATE for the simulation of clinical radiotherapy systems.

References

[1] C.Williams, All about cancer, John Wiley and Sons, 1984

[2] C.J.Karzmark, Medical electron accelerators, McGraw-Hill.Inc., 1993

[3] I.Rabinowitz, J.Broomberg, M.Goitein, Accuracy of radiation field alignment in clinical practice, I.J.Radiat. Oncol. Biol. Phys., Vol 11,p1857-1867, 1985

[4] P.Munro, J.A.Rawlinson, A.Fenster, A digital fluoroscopic imaging device for radiotherapy localization, I.J.Radiat. Oncol. Biol. Phys., Vol 18, p641-649, 1990

[5] J.Leong, Use of digital fluoroscopy as an on-line verification device in radiation therapy, Phys. Med. Biol., Vol. 31, p985-992, 1986

[6] A.G.Visser, H.Huizenga, V.G.M.Althof, et.al., Performance of a prototype fluoroscopic radiotherapy imaging system, I.J.Radiat. Oncol. Biol. Phys., Vol 18, p43-50, 1990

[7] P.Munro, Portal imaging technology : past, present, and future, Seminars in radiation oncology, Vol 5, p115-133, 1995

[8] Geometry and tracking (GEANT4) transport code, http://www.cern.ch/geant4

[10] S.Jan, et al., GATE: a simulation toolkit for PET and SPECT, Phys. Med. Biol., Vol. 49, No. 19, p4543-4561, 2004

[9] J.F.Briesmeister, MCNP-A General Monte Carlo N-Particle Transport Code, Version 4B, LANL Report, LA-12625-M, 1997

[10] P.Metcalfe, T.Kron, P.Hoban, The physics of radiotherapy x-rays from linear accelerator, Medical physics publishing, 1997

[11] G.E.Desorby, A.L.Boyer, Bremsstrahlung review : An analysis of the Schiff spectrum, Med. Phys., Vol. 18, p497-505, 1991

[12] T.Radcliffe, G.Barnea, B.Wowk, et.al., Monte Carlo optimization of metal/phosphor screens at megavoltage energies, Med. Phys., Vol 20, p1161-1169, 1993

[13] D.A.Jaffray, J.J.Battista, A.Fenster, et.al., Monte Carlo studies of x-ray energy absorption and quantum noise in megavoltage transmission radiography, Med. Phys., Vol. 22, p1077-1088, 1995

[14] R.K.Swank, Calculation of modulation transfer functions of x-ray fluorescent screens, Applied Optics, Vol. 12, p1865-1870, 1973

[15] G.Lubberts, Random noise produced by x-ray fluorescent screens, J. Opt. Soc. Am., Vol. 58, p1475-1483, 1968

[16] J.Bissonnette, P.Munro, Evaluation of a high-density scintillating glass for portal imaging, Med. Phy., Vol. 23, p401-406, 1996

[17] G.E.Giakoumakis, C.D.Nomicos, P.X.Sandilos, Absolute efficiency of Gd2O2S:Tb screens under fluoroscopic conditions, Phy. Med. Biol., Vol. 34, p673-678, 1989

[18] G.E.Giakoumakis, C.D.Nomicos, E.N.Yiakoumakis, et.al., Absolute efficiency of rare earth oxysulphide screens in reflection mode observation, Phy. Med. Biol., Vol. 35, p1017-1023, 1990

[19] B.H.Hasegawa, The physics of medical x-ray imaging, Medical physics publishing, 1991

[20] Y.H.Chung, H.K.Kim, G.Cho, S.K.Ahn, , H.K.Lee, and S.C.Yoon, Characterization of X-ray detector for CCD-based electronic portal imaging device, Korean J. Med. Biol. Eng., Vol. 21, 2, p119-127, 2000

[21] R.Rajapakshe, S.Shalev, Noise analysis in real-time portal imaging. I. Quantization noise, Med. Phys, Vol. 21, p1263-1268, 1994